

Biosynthesis, characterization and antivenom activities of *Moringa oleifera* silver nanoparticles: an experimental approach

Adeyi, A. O.^{1*}, Olowookorun, T. O.¹, Ajisebiola, B. S.², Labulo, H. A.³, Adeyi, O. E.⁴ and Ibrahim, H.³

¹Animal Physiology Unit, Department of Zoology, University of Ibadan, Ibadan, Nigeria.

²Department of Zoology, Osun State University, Osogbo, Nigeria.

³Department of Chemistry, Federal University of Lafia, Nasarawa State, Nigeria

⁴Department of Biochemistry, Federal University of Agriculture, Abeokuta, Nigeria

*Corresponding author: Akindele Oluwatosin Adeyi, delegenius@yahoo.com

Received: 04 August, 2023

Revised: 21 November, 2023

Accepted: 19 December, 2023

Keywords: *Moringa oleifera*, Silver nanoparticles, *Echis ocellatus*, Haemorrhage, Envenoming.



© 2023 Zoological Society of Nigeria



This is an Open Access article distributed under the terms of Creative Commons Attribution License 4.0 (CC BY-NC-SA)

Abstract

Moringa oleifera has been previously established to possess neutralizing potentials against *Echis ocellatus* venom. This study however, investigated the bioefficacy of silver nanoparticles biosynthesized from *M. oleifera* leaf extract aimed at improving its bioactivity against *E. ocellatus* venom-induced toxicities using *in vivo* and *in vitro* methods. The intrinsic characteristics of the produced *M. oleifera*-Silver nanoparticles (MO-AgNPs) were carried out using energy dispersive X-ray, X-ray diffraction, scanning electron microscopy, transmission electron microscopy and Fourier-transform infrared spectroscopy. Twenty-five male Wistar rats divided randomly into five groups (n=5) were used for the antivenom study. Group 1 received saline while groups 2 to 5 were envenomed intraperitoneally with 0.22mg/kg (LD₅₀) of *E. ocellatus* venom. Group 2 was left untreated while groups 3 to 5 were treated with 0.2ml of antivenom, 5 and 10mg/kg MO-AgNPs post-envenomation, respectively. Blood and tissue of treated rats were analyzed for hematological parameters and histopathology, respectively. The MO-AgNPs formation was confirmed with a colour change from light brown to yellowish-brown with maximum SPR band at 420nm from UV-Vis analysis, indicating a reflection of the bio-reduction of Ag⁺ to Ag⁰. The Transmission electron micrographs showed well dispersed spherical AgNPs with average particle size of 15.7nm. Treatment with MO-AgNPs caused a significant improvement of acute anemia, leucopenia and thrombocytopenia induced by the venom in the envenomed treated rats. Also, MO-AgNPs inhibited the haemorrhagic, haemolytic and anticoagulant activities of the venom. Tissue lesions observed in heart of envenomed untreated rats were attenuated after treatment with MO-AgNPs. The biosynthesized MO-AgNPs exhibited potent neutralizing potentials than *M. oleifera* crude extract against *E. ocellatus* venom toxicities.

Introduction

Snakebite envenoming poses a typical ravaging occupational and environmental menace, particularly in rustic communities of tropical developing countries (WHO 2015). *Echis ocellatus*, also known as carpet viper is in the Viperidae family, a species liable for numerous clinical complexities of extreme systemic and local pathology (Chippaux 2011). It has been reported that *E. ocellatus* accounts for 60% of fatalities resulting from 90% of bites in sub-Saharan Africa (Yusuf *et al* 2015). This species is commonly found in different parts of Nigeria and its envenoming has reportedly caused numerous deaths, particularly in the North-Eastern region (Harrison *et al* 2003). Envenomation by *E. ocellatus* results in pathophysiological conditions like swelling, blistering, coagulopathy, necrosis, haemotoxicity and haemorrhages (Chippaux 2011) as a result of the presence of toxic enzymes majorly snake venom metalloproteinases (SVMPs) (Harrison *et al* 2003).

For some years now, studies on the treatment of snake envenoming using other remedies of natural or synthetic origins have gained more popularity due to drawbacks in the use of conventional antivenom (de Silva *et al* 2016; Adeyi *et al* 2021a, 2023 and Ajisebiola *et al* 2022, 2023). Also, research interest gaining scientific importance and attention is focus on the utilization of silver nanoparticles (AgNPs) synthesized via the green route, as therapeutic agents most especially the bio-based process, using synthesis with plant extracts (Iravani *et al* 2014; Lee and Jun 2019). AgNPs plant extracts synthesis is generally known as “green synthesis” and its processes are deemed non-toxic, less expensive and environmentally friendly when compared to conventional AgNPs chemical synthesis (Srikanth *et al* 2016). The greener approach towards the synthesis of AgNPs is a novel, promising area of study with robust potential and serve as one of the many bases of potent drugs with excellent prospects to combat many diseases such as cancer, diabetes, inflammation and antimicrobial effects (Ge *et al* 2014). Plant-derived AgNPs have been recognized in the field of nano-medicine owing to their

promising potential in a wide sphere of bio-medical applications and many researchers have demonstrated therapeutics potentials of green synthesized AgNPs as antimicrobial, antibacterial, antifungal and anticancer (Khorrami *et al* 2018; Oves *et al* 2018). The significant potentials and fewer safety concerns of plant-derived AgNPs have prompted diverse research towards harnessing the full potential of AgNPs for treatment in the biomedical field (Wei *et al* 2015). Also, the synthesis of nano-particles utilizing plants gives large-scale options for the production of nanoparticles (Sharma *et al* 2009).

Moringa oleifera (Moringaceae) is a vital medicinal plant cultivated in the tropics and subtropical areas of the world (Irfan *et al* 2021). A lot of pharmacological potentials of *M. oleifera* crude extract have been recorded as anti-inflammatory, anti-diabetic, antihypertensive anti-ulcer, antitumor, antispasmodic, antipyretic, antioxidant (Irfan *et al* 2021) and antivenom (Adeyi *et al* 2021b). Also, the potential therapeutic action of synthesized AgNPs from *M. oleifera* leaf extract has been studied and reported as anticancer (Khor *et al* 2020), antibacterial (Irfan *et al* 2021) and also in insect control (Idowu *et al* 2021). Previous research by Adeyi *et al* (2021) has documented the antivenom efficacy of *M. oleifera* crude extract against *E. ocellatus* envenoming. However, there is dearth of information on the antivenom application of bio-synthesized AgNPs using *Moringa oleifera* leaf extract. This current study aimed at providing insights into the potential increase or otherwise in the antivenom efficacy of biosynthesized AgNPs using aqueous extract of *M. oleifera* leaves against *E. ocellatus* venom induced toxicity.

Materials and methods

Procurement of venom and anti-venom

Lyophilized *E. ocellatus* venom was obtained from the Department of Veterinary Pharmacology and Toxicology, Ahmadu Bello University, Zaria, Nigeria and preserved at 4°C. EchiTAB-Plus (ICP) polyclonal antivenom made by Instiudo Clodomiro Picado in Costa Rica was utilized as drug control for this research.

Collection and preparation of plant extract

Freshly harvested *M. oleifera* plants were identified at the Herbarium of Department of Botany, University of Ibadan, Nigeria with the coupon identification number, UIH-22442. Thereafter, fresh leaves were carefully detached from the plant stalk and rinsed completely and cleaned using double distilled water (DDW). Exactly 10g of the rinsed and air-dried leaves were weighed and put into a 500ml beaker having 300ml DDW and then heated at 100°C for 10 minutes. The fresh aqueous leaf extract was filtered using Whatman filter paper (185m), generating a pale amber-coloured filtrate. The extract was preserved in the laboratory at temperatures range of 25-28°C for further use.

Green synthesis of *M. oleifera* AgNPs (MO-AgNPs)

MO-AgNPs were synthesised according to methods by Labulo *et al* (2016). A measure of 10ml of the leaf extract of *M. oleifera* was added to 40ml of 1mM AgNO₃ at room temperature. The mixture was stored in the dark cupboard for 24 hours and then isolated by centrifuging at 6000rpm for 30 minutes. The clear fluid obtained was disposed and the residue (i.e. nanoparticles) was rinsed twice using DDW and oven dried at 50°C for 45 minutes. Obtained nanoparticles were kept in a 5ml vial tube and labelled MO-AgNPs for further use.

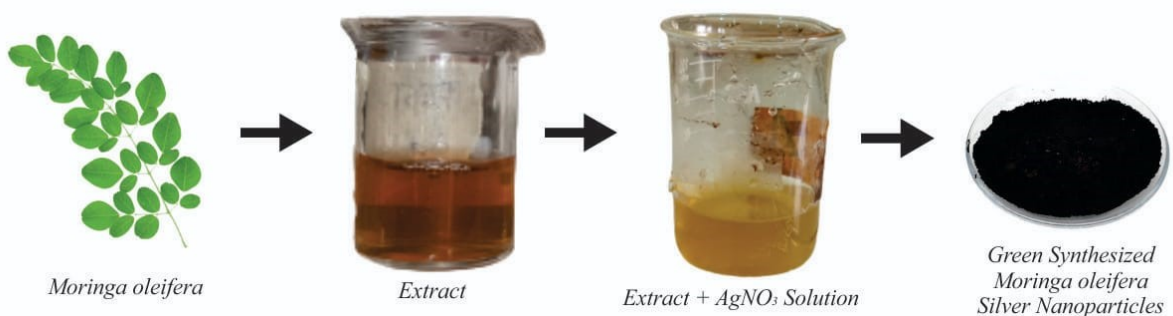


Plate 1. Synthesis of MO-AgNPs

Characterization of MO-AgNPs

Biochrom Libra PCB 1500 Ultra Violet-Vis spectrophotometer was utilised for Surface Plasmon Resonance (SPR) of synthesized MO-AgNPs. AgNPs absorbance evaluation was done by dispersing it in a quartz cuvette with a one-centimetre optical path. This was measured by collecting a small aliquot from the mixture of the reaction and performing a wavelength scan after 24 hours. The inherent characteristics of produced AgNPs were studied using Energy Dispersive

X-ray (EDX), x-ray Power Diffraction (XRD), Fourier Transformed Infrared (FTIR), Scanning Electron Microscope (SEM), Transmission Electron Microscope (TEM), and Thermogravimetric Analysis (TGA). FTIR analysis was carried out with a SHIMADZU FTIR machine with model number IR8400s spectrophotometer, this gave a record for present functional groups and biomolecules found available on the outer layer of MO-AgNPs in the process of synthesis. The surface structures or morphologies and

the elemental constituents of MO-AgNPs were recorded employing EDX (TESCAN Vega TS 5136LM), SEM normally was at 20kV at a working stretch of 20nm. The shapes plus sizes of the MO-AgNPs were examined using Transmission Electron Microscope by plunging an aqueous mixture having the AgNPs onto the carbon-smudged grids with an infrared lamp and for drying. Micrographs were gotten by employing a Philips Morgagni (M-268) working at 80kV. XRD analysis was carried out employing model D8 ADVANCE equipment (Bruker, USA).

Animals and ethical consideration

Twenty-five male albino wistar rats with weight range of 140-160g were acquired from the Department of Zoology, University of Ibadan, Nigeria. They were categorized into five groups each in a well-airy transparent plastic cage at average room temperature. The rats were well fed with regular rat pelletized feed and water *ad libitum*. Animal experiments of this study were approved by the University of Ibadan-Animal Care and Research Ethics Committee (UI-ACUREC), with Assigned number: UI-ACUREC: 18/0108. The processes as stipulated by the ethical board were precisely complied with for proper handling of the animals. National Research Council's guidelines on animal experiments and care were strictly adhered to (National Research Council 2011).

Experimental design

Rats for experimentation were divided into five groups each with five rats (n=5). The first group was administered with normal saline (Normal control), while the second was envenomed and not treated (control venom). Rats in the third group were envenomed and treated with polyvalent antivenom. Also, rats in the fourth and fifth groups were envenomed and treated with 5 and 10mg/kg of MO-AgNPs.

Envenoming and treatment procedures

Rats in the envenomed groups were injected intraperitoneally with 0.2ml of 0.22mg/kg (LD₅₀) of *E. ocellatus* venom dissolved in 1ml of saline (Adeyi *et al.*, 2021). A solution of each dose (5 and 10mg/kg) of MO-AgNPs was prepared in 1ml of saline and given orally to envenomed MO-AgNPs-treated rats while antivenom was administered intravenously to the rats treated with antivenom. The treatment of the animals was done one hour post envenomation for seven consecutive days. Clinical signs of toxicity and mortality were recorded.

Organ and blood sample collection

After seven days of therapy, blood was obtained from the experimental rats through retro-orbital sinus punctation and then collected in bottles containing Ethylene diamine tetraacetic acid (EDTA) for haematological examination. Afterwards, the animals were euthanized by cervical dislocation and dissected according to guidelines by Rowett (1997). The hearts of the experimental rats were collected and stored in 10% formalin for histological examination.

Measurement of haematological indices

Blood samples obtained from the experimental rats were analysed for White Blood Cell (WBC), Packed Cell Volume (PCV), Red Blood Cell (RBC), Haemoglobin (Hb) level, white blood differential counts, and platelet (Baker and Silverton 1985).

In vitro antivenom activity of *M. oleifera*-silver nanoparticles (MO-AgNPs)

Anti-haemorrhagic assay

The procedure reported by Theakston and Reid (1983) was followed for the anti-haemorrhagic assay with slight modifications. Fifteen (15) male wistar rats were randomly divided into 5 groups (n=5). The first group of rats was injected with 0.2ml of saline solution, which was used as control. In the second group, rats were injected with 0.2ml of *E. ocellatus* venom and LD₅₀ solution of 1ml of saline (venom control). In separate tubes, 0.2ml of antivenom and 0.2ml of 5 and 10mg/kg of MO-AgNPs dissolved in 1ml of saline were added to 0.2ml of LD₅₀ venom. The mixtures were incubated at 37°C for an hour. Thereafter, 0.2ml of the prepared solution was administered intradermally into rats in the third, fourth and fifth groups, respectively. The haemorrhagic lesion was observed, measured and recorded after 3 hours.

Anti-haemolytic assay

In the anti-haemolytic assay, 20ml of citrated bovine blood was used, following the method described by Gomes and Pallabi (1999). The erythrocytes were cleaned with 5ml of saline solution (0.9%) and centrifugation at 2400rpm for 10 minutes. This was repeated ten times to obtain free packed cells. After several rinsing with saline, a 10% cell suspension was prepared in normal saline. In separate tubes, 0.2ml of *E. ocellatus* venom LD₅₀ was made to a solution employing 1ml of saline which was combined with 2ml of 10 per cent cell suspension, as well as 0.2ml of 5 and 10mg/ml of MO-AgNPs and polyvalent antivenom (0.2ml) respectively. The control tube for the venom contained 0.2ml of venom and 10% cell suspension. The combinations were prepared in triplicates and incubated at 37°C for 60 minutes. Haemolysis was halted by adding 3mL of cooled phosphate buffer saline (PBS pH 7.2). Solutions in the tubes were centrifuged at 2400rpm for 10 minutes and the absorbance of each supernatant was read at 540nm.

Coagulant assay

For the anticoagulant assay, citrated bovine plasma was used according to the method described by Gomes and Pallabi (1999). Five (5) test tubes were numbered 1-5 each in triplicate. For the control setup, 0.2ml of normal saline was measured into test tube 1. Test tubes 2 to 5 contained an exact dose of 0.2ml LD₅₀ of the venom and 0.2ml of bovine-citrated plasma. Setup in tube 2 was used as the venom control. To test tubes 3 to 5, 0.2ml of 5 and 10mg MO-AgNPs solution in 1ml normal saline and 0.2ml of polyvalent anti-venom were added, respectively. Subsequently, 0.2ml of CaCl₂ was added to all test tubes, and the combination was incubated at

37°C. The clotting time was monitored and recorded for each test tube.

Histopathological evaluation

The heart tissues from the experimental rats were processed routinely for histological examination and stained with hematoxylin-eosin stain according to Drury and Wallington (1980).

Statistical analysis

The data analysis was done using the Statistical software (SPSS version 20). The figures were presented as average \pm standard error (S.E). The relationship between varying groups was analysed using one-way Analysis of Variance (ANOVA), followed by the Duncan Multiple Range Test (DMRT) at $p < 0.05$.

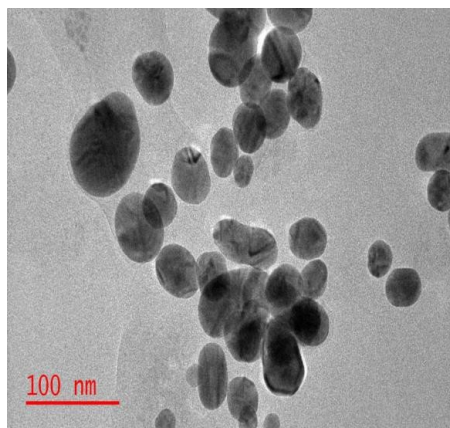
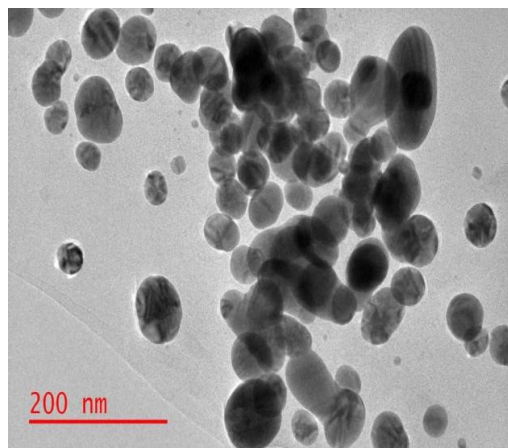
Results

UV-Vis for MO-AgNPs

The formation of the MO-AgNPs was confirmed by a colour transition from light-brown to yellowish-brown as a result of the reaction of *M. oleifera* leaf extract and AgNO_3 solution. This is as a result of the bio-reduction from Ag^+ to Ag^0 , which was observed from the UV-vis spectra (Figure 1). The maximum SPR band was recorded at 420 nm.

Transmission Electron Microscopy and particle size distribution

The TEM micrographs showed aggregated and dispersed spherical AgNPs while some are irregular in shape (Figures 2a and 2b). The average particle size of MO-AgNPs was arithmetically estimated using Debye-Scherrer's equation. Figure 2b indicates an average



Figures 2a and 2b: TEM Micrographs of MO-AgNPs

FTIR analysis

The FTIR spectrum of MO-AgNPs showed peaks at 3303 , 2917 , 2137 , 1619 , and 1021cm^{-1} , showing $-\text{OH}$ group, C-H vibrations, $-\text{C}\equiv\text{C}-$, N-H, and C-O-C functional groups (Figure 5). These peaks suggest that the silver nanoparticles may be surrounded by hydroxyl groups and aliphatic or carboxylic compounds. In addition, the FTIR spectra of the aqueous leave excerpts of *M. oleifera* revealed absorption peaks at 3235cm^{-1} for O-H stretching combined alcohols, 2095.76cm^{-1} for $-\text{C}\equiv\text{C}-$ of the alkyne group, and 1644cm^{-1} for amine

particle size of the dispersed AgNPs of 15.7nm with a polydispersity index (PDI) of 0.186 indicating a stable and colloidal dispersion.

EDX and SEM analyses

The EDX spectrum showed a high intensity for Ag confirming the formation of AgNPs (Figure 3). As a result of the SPR, strong count for metallic nanosilver (61.9%) for other elements (i.e., 0-23.0%, N - 6.6%, S - 4.3%, Fe - 1.3%, Si - 0.9%, Cu - 0.7%, P - 0.6%, Zn - 0.3%, Al - 0.2%, Cr - 0.1%) were recorded. Metallic silver is the highest constituent compared to Si, Fe, Zn and Al. These other elements may come from the biomolecules of *M. oleifera* that are attached to the surface of MO-AgNPs thereby confirming the participation of biomolecules from the plant as stabilizers of the nanostructure (Figure 4).

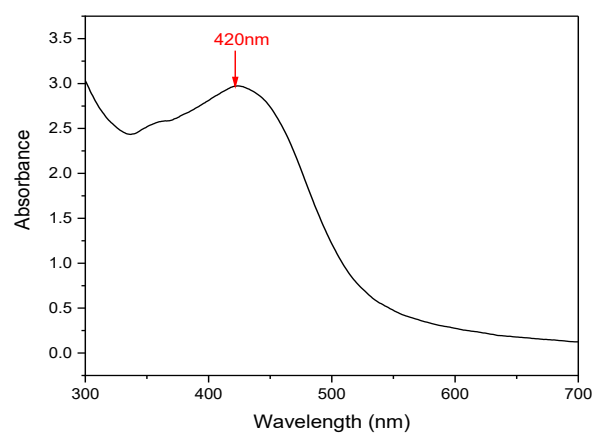


Figure 1. UV-Vis spectra of the synthesized MO-AgNPs

groups present in the proteins. The absorption band at 1644cm^{-1} in the spectra of extract of *M. oleifera* was moved to a lesser frequency of 1619cm^{-1} for MO-AgNPs, indicating amine class are primarily active in the lowering and stabilization of silver ions to AgNPs and prevent agglomeration.

XRD analysis

The crystallinity of MO-AgNPs was affirmed by XRD characterization. Figure 6 indicated the XRD result of the MO-AgNPs at $2(\theta) = 26.3$, 38.6 , 44.2 , and 64.5 . The

calculated average particle size using full-width at half maximum (FWHM) of the (111) and (200) peaks were 19.3 and 22.5nm, respectively.

Observed mortalities from the envenomed animals during treatment with MO-AgNPs

No mortality was recorded in the control rats whereas 20% mortality occurred in the untreated envenomed

group. The envenomed group that was treated with 5mg/kg of MO-AgNPs and antivenom had 10% mortality each, respectively. However, no mortality was recorded in envenomed rats treated with 10mg/kg of MO-AgNPs. Also, clinical symptoms of toxicity shown by the envenomed rats included sluggishness, mild bleeding at the site of venom injection, and reduced physical activities.

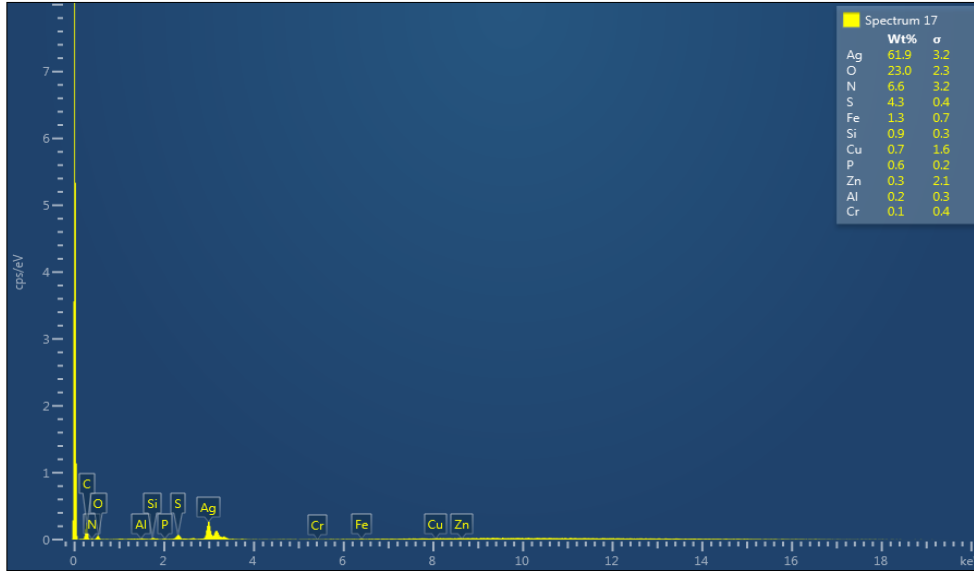


Figure 3: EDX Spectra of MO-AgNPs

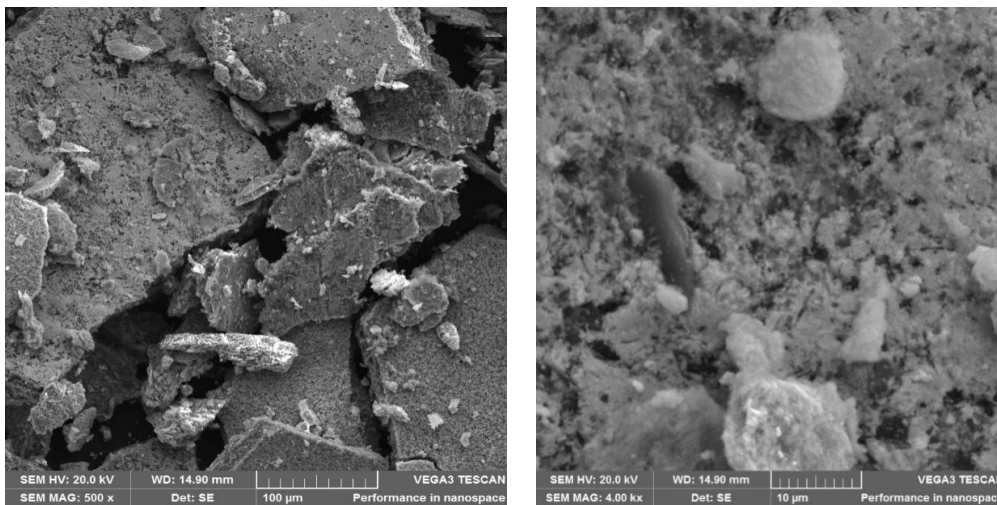


Figure 4: SEM images of MO-AgNPs

In vivo antivenom activity of MO-AgNPs against *E. ocellatus* venom

Haematological parameters of rats envenomed with *E. ocellatus* venom after treatment with MO-AgNPs

The levels of RBC, haemoglobin concentration (Hb), PCV, and platelet counts in the untreated group (venom control) were significantly lower than in the control. Conversely, envenomed rats treated with antivenom and MO-AgNPs showed a substantial increase in PCV, platelet counts, RBC, and Hb, and compared to the venom control. However, dose dependent increase was observed in RBC, PCV counts and Hb concentration of envenomed groups treated with varying concentrations

of MO-AgNPs. It is also noteworthy that PCV, RBC, platelet counts and Hb concentration of the envenomed group treated with 10mg/kg of MO-AgNPs were higher when compared with group treated with antivenom. (Table 1).

WBC and Differentials of the Envenomed treated with MO-AgNPs

The WBC and lymphocytes counts in the envenomed group were significantly lower compared to the control. However, these parameters substantially increased in the envenomed rats treated with antivenom and MO-AgNPs in comparison to the venom control group. Similarly, the values obtained for neutrophils (NEUT), monocytes

(MONO), and eosinophils (EO) were significantly higher in envenomed treated rats compared to the control (Table 2).

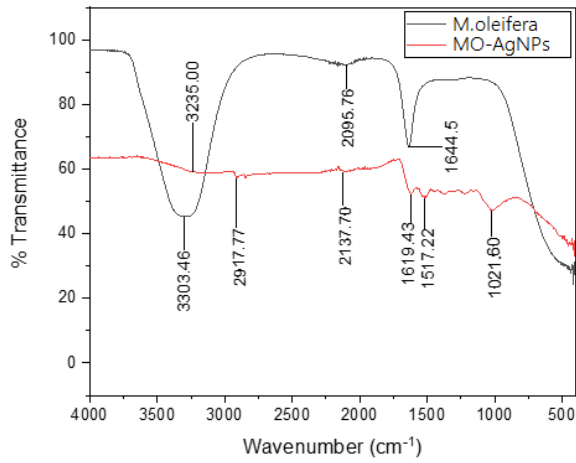


Figure 5. FTIR of Synthesized MO-AgNPs

Antihemorrhagic action of MO-AgNPs

Intradermal injection of *E. ocellatus* venom in rats showed a visible spot with 100% haemorrhage recorded

in the venom control but no lesion was observed in the control rats injected with saline. However, the group injected with the venom and a high dose of MO-AgNPs showed a highly significant inhibition of haemorrhage induced by the venom when compared to groups treated with a low dose of MO-AgNPs and antivenom (Table 3).

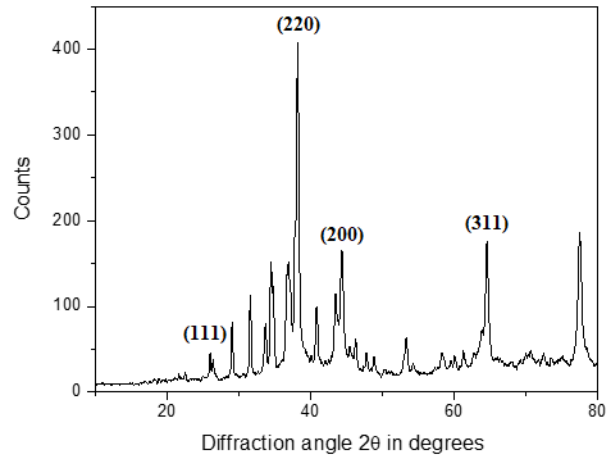


Figure 6: The XRD pattern of MO-AgNPs

Table 1: Haematological parameters of *E. ocellatus* envenomed rats after treatment with MO-AgNPs

Parameters	Group 1 (normal control)	Group 2 (venom control)	Group 3 (venom/antivenom)	Group 4 (venom/5mg MO-AgNPs)	Group 5 (venom/10mg MO-AgNPs)
PCV (%)	48.33±1.33 ^{ab}	39.45±1.55 ^c	42.23±2.13 ^a	44.5±5.1.56 ^a	47.33±1.76 ^{ab}
Hb (g/dl)	16.62±0.45 ^{ab}	12.60±0.65 ^c	14.64±0.63 ^a	15.20±1.90 ^a	16.32±0.55 ^{ab}
RBC (cell/L)	8.43±0.15 ^a	6.32±0.23 ^c	7.75±0.46 ^b	7.78±0.45 ^b	8.10±0.28 ^a
Platelet (×10 ³ cell/l)	109.33±3.08 ^a	100.62±2.88 ^c	104.95±1.05 ^b	106.5±1.52 ^{ab}	108.66±2.67 ^a
MCH (pg/cell)	209.08±1.92 ^b	199.36±1.29 ^a	201.54±4.22 ^b	206.24±2.06 ^b	208.23±1.76 ^b
MCHC (g/dl)	34.85±0.36 ^a	30.3±1.67 ^b	32.5±0.12 ^a	32.64±0.21 ^a	33.58±0.21 ^a
MCV (fl)	629.38±4.79 ^a	617.08±3.25 ^{ab}	618.05±5.72 ^{ab}	620.76±4.45 ^a	626.91±3.30 ^a

Data demonstrated as average ± Standard error means (SEM), (n=3). Figures in similar columns carrying varying superscripts are taken substantial (p<0.05). **HGB:** Hemoglobin, **MCV:** Mean corpuscular volume, **MCH:** Mean corpuscular heamoglobin, **MCHC:** Mean corpuscular hemoglobin concentration

Table 2: Differentials of *E. ocellatus* and WBC envenomed rats post-treatment with MO-AgNPs

Parameters	Group 1 (normal control)	Group 2 (venom control)	Group 3 (venom/antivenom)	Group 4 (venom/5mg MO-AgNPs)	Group 5 (venom/10mg MO-AgNPs)
WBC (×10 ³ cell/l)	2.41±0.14 ^a	1.6±0.12 ^b	2.5±0.05 ^a	2.42±0.37 ^a	2.25±0.07 ^a
Lymphocytes (%)	79.34±0.57 ^a	68.12±2.32 ^b	76.51±3.50 ^a	76.43±1.32 ^a	79.21±1.15 ^a
Neutrophils (10 ³ cm ³)	22.33±0.88 ^a	19.24±1.74 ^b	19.23±3.60 ^a	20.51±4.54 ^a	20.66±1.20 ^a
Monocytes (10 ³ µl)	2.66±0.66 ^a	2.12±1.02 ^b	2.53±0.52 ^a	2.46±1.04 ^a	2.33±0.33 ^a
Eosinophils (10 ³ µl)	2.45±0.57 ^a	1.32±0.45 ^b	2.61±0.36 ^a	2.53±0.52 ^a	2.45±0.57 ^a

Data demonstrated as average ± Standard error means (SEM), (n=3). Figures in similar columns with varying superscripts are seen as substantial (p<0.05)

Antihaemolytic activity of MO-AgNPs

The control setup had 100% haemolysis as the venom exhibited conventional hemolysis of bovine red blood cells. However, haemolysis induced by the venom was

strongly inhibited by the high dose of MO-AgNPs and antivenom (Table 4).

Coagulation activity of MO-AgNPs

The control sample clotted within 50s, whereas the venom prolonged the clotting time to 292s in venom

control setup. However, the setup treated with high dose of MO-AgNPs and antivenom substantially ($p < 0.05$) reduced the clotting time to 68 and 60 s, respectively (Figure 7).

Histopathological observation of the heart of the envenomed treated rats

Heart of control rats indicated regular formation of cardiomyocytes without observable defects while slides prepared from the heart tissues of venom control indicates moderate foci of interstitial cell hyperplasia, haemorrhage, and hypertrophy of myofibres. The observed morphological alterations were extenuated in groups envenomed and those treated with antivenom and MO-AgNPs (Plate 2).

Table 3. Inhibition of haemorrhagic action by MO-AgNPs

Therapy	Percentage inhibition (%)
Group 1 (Saline)	No lesion
Group 2 (Venom only)	0 (100% haemorrhage)
Group 3 (Venom/antivenom)	62.00±2.42 ^a
Group 4 (Venom/5mg/kg MO-AgNPs)	64.00±2.68 ^a
Group 5 (Venom/10mg/kg MO-AgNPs)	82.00±3.21 ^b

Data demonstrated as average ± Standard error means (SEM), (n=3). Figures in similar columns with varying superscripts are considered substantial ($p < 0.05$)

Table 4. Inhibition of hemolytic action by MO-AgNPs

Therapy	Percentage inhibition (%)
Group 1 (Normal control)	0 (100% haemolysis)
Group 2 (Venom control)	26.00±1.45 ^a
Group 3 (Venom/antivenom)	82.00±2.24 ^b
Group 4 (Venom/5mg/kg MO-AgNPs)	68.00±2.00 ^a
Group 5 (Venom/10mg/kg MO-AgNPs)	78.00±2.86 ^b

Data are demonstrated as average±Standard error means (SEM), (n=3). Figures in similar columns with varying superscripts are considered substantial ($p < 0.05$)

Discussion

The field of nanotechnology has turned into an important domain in medical sciences due to its great potentials and utilization for treatment of many chronic diseases by researchers most especially the use of phytoconstituents as valuable candidates in synthesizing green silver nanoparticles (AgNPs) (Jain *et al* 2021). Reports abound that metal combined with entire-plant extracts would better potentiate the activities of the phytoconstituents (Chaudhary and Singh 2010; Gomes *et al* 2016; Hingane *et al* 2018). Recently, the application of metal nanoparticles and nano-based bio-products in the sphere of biomedicine is gaining more research attention and has paved way for capable drug molecules (Gomes *et al* 2016; Hingane *et al* 2018).

The MO-AgNPs revealed diagnostic peak characteristics of present functionalities that caused a decline of Ag^+ to afford the Ag^0 . Also, aliphatics amine,

carbonyl of amide, and hydroxyl are characteristic functionalities that were noticed and the manifestation of the outer layer functionality examination means functional groups presence can reduce the Ag^+ , and also cause the stabilization of MO-AgNPs which is in tandem with report of Idowu *et al* (2021).

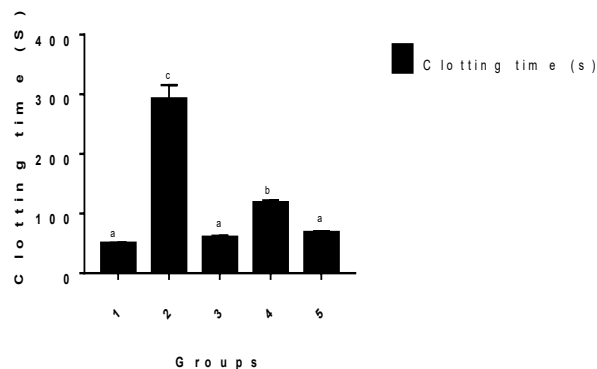


Figure 7. Coagulant activity of MO-AgNPs against *E. ocellatus* venom

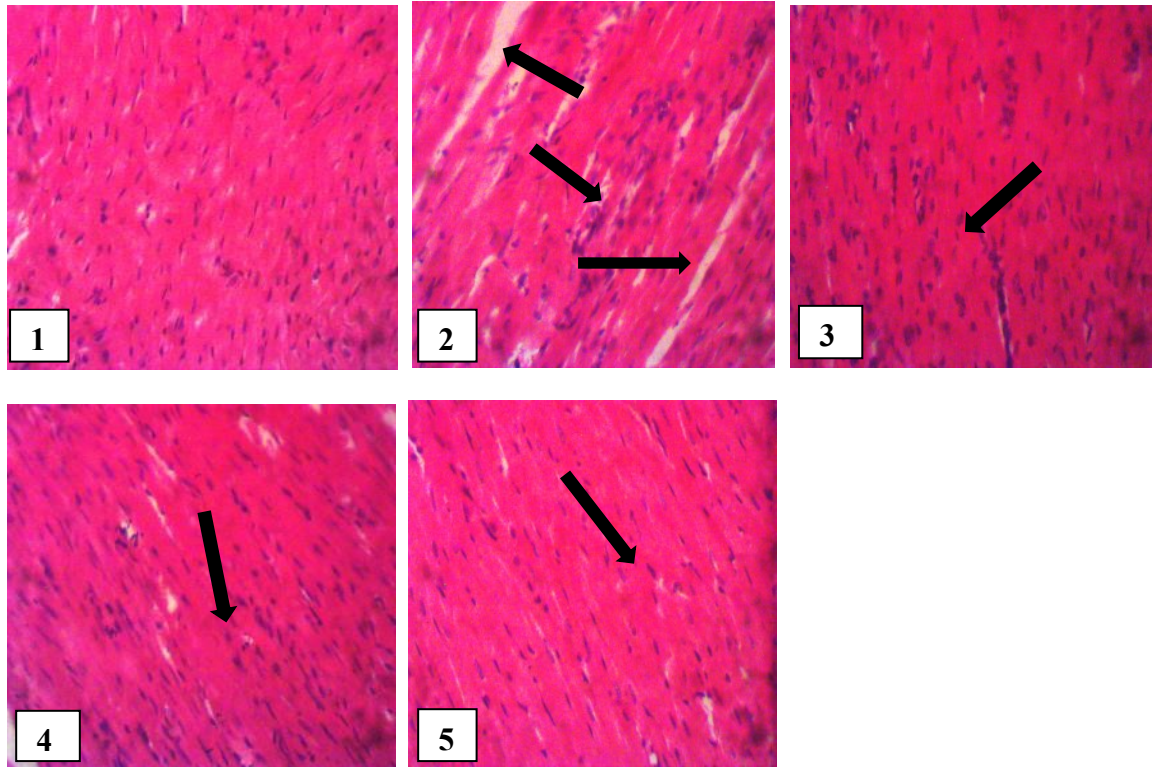
Group 1: Dionised water/citrated plasma/CaCl₂ (regular control), **Group 2:** Venom/citrated plasma/CaCl₂ (Venom control), **Group 3:** Venom/citrated plasma/CaCl₂/0.2ml anti-venom, **Group 4:** Venom/citrated plasma/CaCl₂/5 mg/kg of MO-AgNPs, **Group 5:** Venom/citrated plasma/ CaCl₂/10 mg/kg of MO-AgNPs. Data are demonstrated as average ± Standard Error Means (SEM), (n=3). Figures in similar columns with varying superscripts are considered substantial ($p < 0.05$)

The corresponding single peak absorbance spectra of MO-AgNPs could be attributed to feature vibrations due to disparity in the electronic energy levels of AgNPs. The maximum SPR band was localized around 420nm, the same as the wavelength absorption band of a single metallic Ag^0 (Idowu *et al* 2021; Patil and Ashok 2021). The average particle size distribution of the MO-AgNPs was found to be 15.7nm, which is similar to findings from other works using aqueous leave extract of *M. oleifera* (Awwad *et al* 2012; Jayshree and Nallamuthus 2016; Shousha *et al* 2019).

Snake venoms most especially viper venoms contain hydrolytic proteins and enzymes that manifest toxic actions resulting in clinical complications (Hamza *et al* 2010). These proteins may cause haematological disturbances, damage blood capillaries and induce haemorrhage through their associated proteins and changed the primary hemostasis by disrupting platelet adhesion (Cherifi and Laraba-Djebari 2013). As observed in this study, *E. ocellatus* venom altered the haematological indices by inducing acute anaemia and thrombocytopenia. Finding also showed induced leucopenia in the venom control rats as levels of WBC and differentials significantly decreased and these are vital components of the blood. Leucopenia induced by the venom may be a result of bone marrow failure, tumour and collagen vascular diseases (Al-Sadoon and Fahim 2012) which could diminish the ability of the body cells to fight body foreign invaders that can cause infections.

Furthermore, *E. ocellatus* venom induced various histopathological alterations in heart of the envenomed untreated rats as moderate foci of interstitial cell hyperplasia, haemorrhage, and hypertrophy of myofibres were noticed. Cardiac lesions is one of the pathological effects associated with snakebite envenoming as a result of cardiotoxin(s) and PLA₂

leading to cytotoxicity and cellular necrosis (Asad *et al* 2014). Additionally, SVMPs present in viper venom are considered liable for regular haemorrhage, reducing the constituent of the vascular basement membrane, and leading to dislodgement of the vascular structure (Silveira *et al* 2004; Fox and Serrano 2005).



H.E. ×400

Plate 2. Histopathology of the heart tissues of envenomed treated rats.

Group 1 (Control): Regular cardiomyocytes with no observable defect, **Group 2 (Venom control):** There are foci of moderate interstitial cell hyperplasia, haemorrhage, and hypertrophy of myofibres, **Group 3 (Venom/antivenom):** Moderate interstitial cell hyperplasia and hypertrophy of myofibres, **Group 4 (Venom/5mg/kg MO-AgNPs):** Mild hypertrophy of myofibres, **Group 5 (Venom/10mg/kg MO-AgNPs):** Mild hypertrophy of myofibres.

The manifestations of pathophysiology as observed in the envenomed untreated rats are evidence of the toxic actions exhibited by viper venom toxins as earlier reported in envenomed animals (Al-Sadoon and Fahim 2012; Adeyi *et al* 2021; Ajisebiola *et al* 2021) and in viper envenomed victims (Netto *et al* 2004). However, treatment with a low and high dose of MO-AgNPs significantly improved the haematological indices dose-dependently and ameliorated the pathological defects noticed in the heart of envenomed treated rats. The observed improvement could be attributed to the neutralizing potentials of MO-AgNPs after treatment as studies have reported the neutralizing potency of silver nano particles-based plant extract against venoms of snake species (Singh *et al* 2020; Ghosh *et al* 2021).

Phospholipase A₂ (PLA₂) and SVMPs are widespread proteins that constitute Viperidae venom. The latter is known to cause hemostasis disturbance by

hydrolyzing fibrinogen or degrading the fibrin clot and wall of blood capillaries thereby enhancing the haemorrhagic effect resulting in spontaneous pathological bleeding (Al-Sadoon and Fahim 2012) while the former hydrolyzes cell membrane and blood cells resulting in tissue necrosis and haemolysis (Lomonte *et al* 2003). The results showed that, *E. ocellatus* venom displayed complete haemorrhagic action in the venom control rats as expected of viper venom which was in tandem with earlier study (Adeyi *et al* 2021). Also, the venom-induced direct haemolysis on citrated bovine erythrocytes and prolonged blood coagulation could be attributed to the action of SVMPs and PLA₂ enzymes respectively (Adeyi *et al* 2021; Ajisebiola *et al* 2021). In this study, MO-AgNPs effectively countered the haemorrhagic and blood-lytic activities of the venom and restored coagulation by shortening the clotting time.

As earlier stated, our previous study has reported the antivenom effects of crude extract of *M. oleifera* at a high dose of 600 mg/kg as to *E. ocellatus* venom toxicities *in vitro* and *in vivo* (Adeyi *et al* 2021) whereas, findings from this study demonstrated successful neutralization of the venom *in vitro* and *in vivo* by MO-AgNPs at a high dose of 10 mg/kg thereby, confirming the antivenom potentials of MO-AgNPs and indicating that biosynthesized silver nano-particles with plant extract possess more potent antivenom activity than a whole-plant extract, and this observation corroborated with Singh *et al* (2020).

The mechanism of MO-AgNPs inhibitory action against the venom toxic activities is fully unknown yet but it should be noted that successful use of plant biosynthesized silver nanoparticles using *M. oleifera* extract against some diseases has been reported (Idowu *et al* 2021; Irfan *et al* 2021; Khor *et al* 2020). The possible mechanism of AgNP's successes in the treatment of diseases may be due to the unique electrical and magnetic properties including their capability to merge biomolecules, high layer area to volume ratio, significant upper layer reactivity, ease of synthesis and characterization, low cytotoxicity, and potential to enhance gene expression for redox processes (Luis *et al* 2020).

Report showed that phenolic, alkaloids, enzymes, coenzymes, proteins sugars and terpenoids are the main phytochemicals that are liable for the bioreduction of Ag salts (Roy *et al* 2019). *M. oleifera* leaf is a great source of tannins, flavonoids, phenolic compounds, alkaloids and terpenoids (Vergara-Jimenez *et al* 2017) and successful bioreduction of silver and transformation of silver ions to nanoparticles were achieved as relevant contributions of these functional groups (Singh *et al* 2019). Another possible mechanism of the antivenom effects exhibited by green synthesis MO-AgNPs could be attributed to the synergistic effect between the MO-AgNPs and the biological coating of the plant excerpts on the outer layer of the nanoparticle (Khorrami *et al* 2018).

Conclusion

This study reported the successful bio-synthesis of Ag nanoparticles employing aqueous extracts of *M. oleifera* and its antivenom bioactivity against *E. ocellatus* venom toxicities *in vivo* and *in vitro*. This study affirmed that venom MO-AgNPs have great potential as an antidote against snake venom toxicities when compared to the *M. oleifera* crude extract and could be used as part of an integrated approach towards effective treatment of snakebite envenoming. However, further study is required in understanding the mechanism of MO-AgNPs in countering venom's toxic effects.

Acknowledgements

Not applicable

Conflict of Interest statement

All authors declare no conflict of interest.

References

- Adeyi, A.O., Mustapha, K. K., Ajisebiola, B.S., Adeyi, O. E., Damilohun, S. M. and Okonji, R. E. 2021a. Inhibition of *Echis ocellatus* venom metalloprotease by flavonoid-rich ethyl acetate sub-fraction of *Moringa oleifera* leaves (Lam): *in vitro* and *in silico* approaches. *Toxin Rev.* 40: 1-12.
- Adeyi, A.O., Adeyemi, S.O., Effiong, E.O.P., Ajisebiola, B.S., Adeyi, O.E. and James, A.S. 2021b. *Moringa oleifera* extract extenuates *Echis ocellatus* venom-induced toxicities, histopathological impairments and Inflammation via enhancement of Nrf2 expression in rats. *Pathophysiology* 28: 98-115.
- Adeyi, A.O., Abideen, O.J., Ajisebiola, B.S., Adeyi, O.E., Damilohun, S. M. and Okonji, R. E. 2023. Inhibition of phospholipases from *Naja haje* and *Naja nigricollis* venoms by active fraction of *Moringa oleifera* leaves using *in vitro* and *in silico* methods *Toxin Rev.* 42: 1-12.
- Ajisebiola, B.S., Rotimi, S., Anwar, U. and Adeyi, A.O. 2021. Neutralization of *Bitis arietans* venom-induced pathophysiological disorder, biological activities and genetic alterations by *Moringa oleifera* leaves. *Toxin Rev.* 40: 847-858.
- Ajisebiola, B.S., Bello, F.T., Osamudiamen, P.M., Oladele, J. O. and Adeyi, A.O. 2023. Inhibition of metalloproteinase from *Bitis arietans* venom *in vitro* by the ethyl acetate fraction of *Moringa oleifera* and its chemical profile. *Rev. Bras. Farmacogn.* <https://doi.org/10.1007/s43450-023-00416-4>.
- Al-Sadoon, M.K. and Fahim, A. 2012. Possible recovery from an acute envenomation in male rats with LD50 of *Echis coloratus* crude venom: I-A seven days hematological follow-up study. *Saudi J Biol. Sci.* 19: 221-227.
- Asad, M.H., Murtaza, G., Ubaid, M., Durre, S., Sajjad, A., Mehmood, R., Mahmood, Q., Ansari, M.M., Karim, S., Mehmood, Z. and Hussain, I. 2014. *Naja naja karachiensis* envenomation: biochemical parameters for cardiac, liver, and renal damage along with their neutralization by medicinal plants. *Biomed. Res. Int.* 970540.
- Awwad, A.M. and Nidà, M.S. 2012. 'Green Synthesis of Silver Nanoparticles by Mulberry Leaves Extract'. *J. Nanosci. Nanotechnol.* 2(4): 125-28.
- Baker, F.T. and Silverton, R.E. 1985. Introduction to Medical Laboratory Technology, Butterworth, London, p. 408, 0407732527.
- Chaudhary, A. and Singh, N. 2010. Herbo mineral formulations (Rasaoushadhies) of Ayurveda an amazing inheritance of Ayurvedic pharmaceuticals. *Anc. Sci. Life.* 30: 18-26.
- Cherifi, F. and Laraba-Djebari, F. 2013. Isolated biomolecules of pharmacological interest in hemostasis from *Cerastes cerastes* venom. *J Venom Anim. Toxins Incl. Trop. Dis.* 19(1): 11. <https://doi: 10.1186/1678-9199-19-11>.

- Chippaux, J.P. 2011. Estimate of the burden of snakebites in sub-Saharan Africa: A meta-analytic approach. *Toxicon* 64: 34-48.
- de Silva, H.A., Ryan, N.M. and de Silva, H.J. 2016. Adverse reactions to snake anti-venom, and their prevention and treatment. *Br. J. Clin. Pharmacol.* 81: 446–452.
- Drury, R.A.D. and Wallington, E.A. 1980. Carleton's Histological Technique. Oxford University 5th Edition, Press, New York, 195.
- Fox, J.W. and Serrano, S.M. 2005. Structural considerations of the snake venom metalloproteinases, key members of the M12 reprolysin family of metalloproteinases. *Toxicon* 45: 969-985.
- Ge, L., Li, Q., Wang, M., Ouyang, J., Li, X. and Xing, M.M.Q. 2014. Nanosilver particles in medical applications: synthesis, performance, and toxicity. *Int. J. Nanomed.* 9: 2399-2407.
- Ghosh, R., Sarkhel, S., Saha, K., Parua, P., Chatterjee, U. and Mana, K. 2021. Synthesis, characterization & evaluation of venom neutralization potential of silver nanoparticles mediated *Alstonia scholaris* Linn bark extract. *Toxicol. Rep.* 8: 888–895.
- Gomes, A. and Pallabi D. (1999). Hannahpep: A Novel Fibrinolytic Peptide from the Indian King Cobra (*Ophiophagus hannah*) Venom. *Biochem. Biophys. Res. Commun.* 266: 488-491.
- Gomes, A., Sengupta, J., Ghosh, S. and Gomes, A. 2016. Application of gold nanoparticle conjugation with 2-hydroxy-4-methoxy benzoic acid (HMBA) from *Hemidesmus indicus* root enhancing neutralization of snake (Viper) venom activity. *J Nanosci Nanotechno* 16: 8322-9. doi: 10.1166/jnn.2016.11777.
- Hall, B.D., Ugarte, D., Reinhard, D. and Monot, R. 1995. Calculations of the Dynamic Debye–Scherrer Diffraction Patterns for Small Metal Particles. *Chem. Phys* 103(7): 2384-94.
- Hamza, L., Gargioli, C., Castelli, S., Rufini, S. and Laraba-Djebari, F. 2010. Purification and characterization of a fibrinogenolytic and hemorrhagic metalloproteinase isolated from *Vipera lebetina* venom. *Biochimie* 92: 797- 805.
- Harrison, R.A., Oliver, J., Hasson, S.S., Bharati, K. and Theakston, R.D.G. 2003. “Novel sequences encoding venom C-type lectins are conserved in phylogenetically and geographically distinct *Echis* and *Bitis* viper species,” *Gene* 315(1-2): 95-102.
- Hingane, V.C., Pangam, D. and Dongre, P.M. 2018. Inhibition of crude viper venom action by silver nanoparticles: a biophysical and biochemical study. *Biophys Physicobiology* 15: 204-13. doi: 10.2142/biophysico.15.0_204.
- Idowu, E.T., Adeogun, A.O., Adams, L.A., Yusuf, M.A., Salami, O.W., Kanmi, O.A., Bello, J.A., Fagbohun, I.K., Otubanjo, O.A. and Awolola, T.S. 2021. Larvicidal potential of two silver nanoparticles (*Moringa oleifera* and *Ficus exasperata*) against laboratory and field strains of *Anopheles gambiae* (Diptera: Culicidae) in Lagos, Nigeria. *JoBAZ* 82: 7 <https://doi.org/10.1186/s41936-020-00204-9>.
- Iravani, S., Korbekandi, H., Mirmohammadi, S.V., Zolfaghari, B. 2014. Synthesis of silver nanoparticles: chemical, physical and biological methods. *Res. Pharm. Sci.* 9(6): 385-406.
- Irfan, M., Munir, H. and Ismail, H. 2021. *Moringa oleifera* gum based silver and zinc oxide nanoparticles: green synthesis, characterization and their antibacterial potential against MRSA. *Biomater. Res* 25: 17.
- Jain, N., Jain, P., Rajput, D. and Patil, U.K. 2021. Green synthesized plant-based silver nanoparticles: therapeutic prospective for anticancer and antiviral activity. *Micro and Nano Syst. Lett.* 9: 5.
- Jayshree, A. and Nallamuthu, T. 2016. ‘Green Synthesis of Silver Nanoparticles: Characterization and Determination of Antibacterial Potency’. *Appl. Nanosci.* 6(2): 259-65.
- Khor, K.Z., Joseph, J., Shamsuddin, F., Lim, V., Moses, E.J. and Samad, N.A. 2020. The Cytotoxic Effects of *Moringa oleifera* Leaf Extract and Silver Nanoparticles on Human Kasumi-1 Cells. *Int. J. Nanomedicine.* 15: 5661-5670.
- Khorrami, S., Zarrabi, A., Khaleghi, M., Danaei, M. and Mozafari, M.R. 2018. Selective cytotoxicity of green synthesized silver nanoparticles against the MCF-7 tumor cell line and their enhanced antioxidant and antimicrobial properties. *Int J Nanomedicine* 13: 8013–8024. <https://doi:10.2147/IJN.S189295>.
- Labulo, A.H., Adesuji, T.E., Oseghale, C.O., Omojola, J., Bodede, O.S., Dare, E.O., Akinsiku, A.A. 2016. ‘Biosynthesis of Silver Nanoparticles Using *Garcinia Kola* and Its Antimicrobial Potential’. *AJPAC* 10(1): 1-7.
- Lee, S.H., and Jun, B.H. 2019. Silver nanoparticles: synthesis and application for nanomedicine. *Int. J. Mol. Sci.* 20(4). <https://doi:10.3390/ijms20040865>.
- Lomonte, B., Angulo, Y. and Calderón, L. 2003. An overview of lysine-49 phospholipase A2 myotoxins from crotalid snake venoms and their structural determinants of myotoxic action. *Toxicon.* 42: 885-901.
- Luis, C., Alfaro-Aguilar, K., Ugalde-Álvarez J., Vega-Fernández, L., de Oca-Vásquez GM. and Vega-Baudrit, J.R. 2020. Green Synthesis of Gold and Silver Nanoparticles from Plant Extracts and Their Possible Applications as Antimicrobial Agents in the Agricultural Area. *J. Nanomater.* 10: 1763; <https://doi:10.3390/nano10091763>.
- National Research Council 2011. Guide for the Care and Use of Laboratory Animals; 8th Edition, National Academies Press: Washington, DC, USA, p. 246.
- Netto, D.P., Chiacchio, S.B., Bicudo, P.L., Alfieri, A.A., Balarim, M.R.S. and Nascimento, N. 2004. Hematological changes in sheep inoculated with natural and Cobalt60-irradiated *Crotalus durissus terrificus* venom (Laurenti, 1768). *J. Venom Anim. Toxins. Incl. Trop. Dis.* 10: 34-52.

- Oves, M., Aslam, M., Rauf, M.A., Qayyum, S., Qari, H.A., Khan, M.S., Alam, M.Z., Tabrez, S., Pugazhendhi, A. and Ismail, I.M.I. 2018. Antimicrobial and anticancer activities of silver nanoparticles synthesized from the root hair extract of *Phoenix dactylifera*. *Mater. Sci. Eng. C* 89: 429-443. <https://doi.org/10.1016/j.msec.2018.03.035>.
- Patil, R.B. and Ashok, D.C. 2021. 'On the Shape Based SPR of Silver Nanostructures'. *Int. J. Nanotechnol.* 18(11-12): 1015-27.
- Rowett, H.G.O. 1997. *Dissecting Guides of Rats with Notes on Mouse*. 111, Bulter and tanner LTD., London, pp. 5-23.
- Roy, A., Bulut, O., Some, S., Mandal, A.K. and Yilmaz, M.D. 2019. Green synthesis of silver nanoparticles: biomolecule-nanoparticle organizations targeting antimicrobial activity. *RSC Adv* 9: 2673-2702.
- Sharma, V.K., Yngard, R.A. and Lin. Y. 2009. Silver nanoparticles: green synthesis and their antimicrobial activities. *Adv. Colloid Interface Sci.* 145: 83-96, <https://doi.org/10.1016/j.cis.2008.09.002>.
- Shousha, W.G., Aboulthana, W.M., Salama, A.H., Mahmoud, H.S. and Ehab, A.E. 2019. Evaluation of the biological activity of *Moringa oleifera* leaves extract after incorporating silver nanoparticles, in vitro study. *Bull. Natl. Res. Cent.* 43: 212. <https://doi.org/10.1186/s42269-019-0221-8>.
- Silveira, K.S., Boechem, N.T., do Nascimento, S.M., Murakami, Y.L., Barboza, A.P., Melo, P.A., Castro, P., de Moraes, V.L., Rocco, P.R. and Zin, W.A. 2004. Pulmonary mechanics and lung histology in acute lung injury induced by *Bothrops jararaca* venom. *Respir. Physiol. Neurobiol.* 139: 167-177.
- Singh, P., Yasir, M., Khare, R. and Shrivastava, R. 2020. Green synthesis of silver nanoparticles using Indian male fern (*Dryopteris Cochleata*), operational parameters, characterization and bioactivity on *Naja naja* venom neutralization. *Toxicol. Res.* 9: 706-713. <https://doi.org/10.1093/toxres/tfaa070>.
- Singh, R., Gupta, A.K., Patade, V.Y., Balakrishna, G., Pandey, K. and Antaryami, S. 2019. Synthesis of silver nanoparticles using extract of *Ocimum kilimandscharicum* and its antimicrobial activity against plant pathogens. *SN Appl. Sci.* 1: 1652. <https://doi.org/10.1007/s42452-019-1703-x>.
- Srikar, S.K., Giri, D.D., Pal, D.B., Mishra, P.K. and Upadhyay, S.N. 2016. Green synthesis of silver nanoparticles: a review. *Green Sustain. Chem.* 06(1): 34-56. doi:10.4236/gsc.2016.61004.
- Theakston, R.D.G. and Reid, H.A. 1983. Development of simple standard assay procedures for the characterisation of snake venoms. *Bull. WHO* 61: 949-956.
- Vergara-Jimenez, M., Almatrafi, M.M. and Fernandez, M.L. 2017. Bioactive Components in *Moringa oleifera* Leaves Protect against Chronic Disease. *Antioxidants* 6:91.
- Wei, L., Lu, J., Xu, H., Patel, A., Chen, Z.S. and Chen, G. 2015. Silver nanoparticles: synthesis, properties, and therapeutic applications. *Drug Discov. Today.* 20(5): 595-601.
- World Health Organisation. Neglected tropical diseases, 2015. snakebite. Accessed 29 October, 2022. http://www.who.int/neglected_diseases/en/.
- Yusuf, P.O., Mamman, M., Ajagun, E., Suleiman, M.M., Kawu, M.U., Shittu, M., Isa, H.I., Tauheed, M. and Yusuf, A. 2015. Snakes Responsible for Bites in North-Eastern Nigeria—A Hospital Based Survey. *J. Environ. Sci. Toxicol. Food Technol.* 9(9): 118-121.